Environ. Sci. Technol. **2007**, *41,* 1646−1652

Electronic Polarizability as a Predictor of Biodegradation Rates of Dimethylnaphthalenes. An *Ab Initio* and Density Functional Theory Study

VITO LIBRANDO* AND ANDREA ALPARONE

Research Centre for Analysis, Monitoring and Minimization Methods of Environmental Risk, c/o Department of Chemistry, University of Catania, viale A. Doria 8, 95125 Catania, Italy

Geometries, relative stabilities, electronic excited states, atomic charges, and electronic dipole polarizabilities of dimethylnaphthalene (DMN) isomers have been calculated in gas and aqueous phases by *ab initio* and DFT methods. At the highest levels of calculation, α,α-DMN (2,6-DMN, 2,7-DMN, and 2,3-DMN) are the lowest energy isomers, while 1,8-DMN is the less stable by 7−8 kcal mol^{-1}. The averaged electronic polarizability, $<\alpha>$, is dependent on the position of the methyl substituents, increasing in the order α,α-DMN < α,β-DMN < β,β-DMN, with the largest values being obtained for 2,6-DMN and 2,7-DMN, while the lowest value is calculated for 1,8-DMN isomer. Polarizability differences among the isomers have been related to their spectroscopic properties. The computed $<\alpha>$ value of DMN isomers, with the notable exception of 2,7-DMN, is in excellent linear relationship with the observed first-order biomass-normalized rate coefficient, a parameter related to the rate of biodegradation of polycyclic aromatic hydrocarbons (PAHs). This result suggests that electronic polarizability may be a useful tool for prediction of biodegradation trends of series of compounds, and inductive and dispersive interactions play a fundamental role in the biodegradation process of DMNs. The present approach is potentially suitable for applications on PAHs with higher molecular weight.

Introduction

Polycyclic aromatic hydrocarbons (PAHs) constitute a group of widespread pollutants of great environmental interest (*1*, *2*). It is widely recognized that PAHs and their metabolites are among the most toxic, carcinogenic, and mutagenic atmospheric contaminants (*3*−*6*). PAHs can be produced from both natural and human activities as a result of incomplete combustion or pyrolysis and there is clear evidence of presence of PAHs in many astronomical objects (*7*−*9*). Due to their ubiquity, it is important to establish effective methodologies for the removal of PAHs from soil and aqueous environments (*10*), mainly based on knowledge and determination of biodegradation constants (*11*).

Great attention has also been directed toward the study of alkylated PAH compounds which are prevalent in PAHs environmental mixtures (*12*−*14*). It is known that degradation rates are noticeably influenced by the position of the alkyl substituents (*15*−*18*). In a recent study, Wammer and Peters (*19*), using a group of aerobic PAH-degraders obtained from a bacterial culture, have determined biodegradation rates represented by first-order biomass-normalized rate coefficients, k_b, of a series of 22 PAHs including some dimethylnaphthalenes (DMN) (1,2-DMN, 1,3-DMN, 1,4-DMN, 1,5-DMN, 1,6-DMN, 1,8-DMN, 2,6-DMN, 2,7-DMN). Biochemical degradation of DMNs proceeds preferentially through addition of one oxygen atom to methyl substituent, producing the corresponding benzylic alcohols (*20*). These reactions are predicted to be thermodynamically favored (*21*). In this series of DMNs, it has been found that the biodegradation rates vary up to 1 order of magnitude, depending on the substituent position. Using a theoretical approach, it has been recently hypothesized that the presence of substituent in α position increases the width of the terminal ring by ca. 1 Å, reducing the binding affinity with the reactive site of the PAH-degrading enzyme (naphthalene dioxygenase) and as a consequence the biodegradative activity (*21*). Thus, the natural logarithm of k_b has been correlated to the calculated average terminal compound width, with the last parameter being proposed as possible descriptor of the biodegradation rate of alternant PAHs (*21*). It should be noted that the binding cavity of the investigated enzyme is almost constituted by hydrophobic residues (*21*), and the rate-determining step of biodegradation is expected to be governed by inductive and dispersive interactions, which depend on the polarizability of the system. Dipole polarizability, α, is a fundamental physical property which measures the charge distribution deformability of an electronic system under the application of weak external electric fields (*22*−*24*). It is involved in many important physical and chemical phenomena (*25*) and can be obtained experimentally (*26*) and also evaluated by computational methods (*27*). Recently, electronic polarizabilities of polychlorinated dibenzo-*p*-dioxins (*28*, *29*) and polychlorinated dibenzofurans (*30*) have been calculated in order to explore ligand−receptor binding behavior as a function of chlorine atom positions; furthermore, computed α values have been correlated to vapor pressures and octanol−air partition coefficients of chlorinated organic nonpolar compounds (*31*).

In this work we report *ab initio* and density functional theory computations of the structure, electronic polarizability, atomic charges, and singlet excited states of DMN isomers 1,2-DMN, 1,3-DMN, 1,4-DMN, 1,5-DMN, 1,6-DMN, 1,7-DMN, 1,8-DMN, 2,3-DMN, 2,6-DMN, and 2,7-DMN. The aim is to investigate the effects of methyl substituents on these properties and explore possible correlations with the biodegradation rates recently published (*19*).

Computational Methods

Geometries of dimethylnaphtalene (DMN) isomers were fully optimized by *ab initio* Hartree−Fock (HF) (*32*) and Møller−Plesset second-order perturbation theory (MP2) (*32*), as well as density functional theory (DFT) (*33*, *34*), employing hybrid B3LYP functional (*35*, *36*) with split-valence polarized Pople's 6-31G* basis set (*32*). For every α,α−, α,β−, β,β−DMN isomer, possible rotamers in the potential energy surface (PES) around the C−CH_3 bonds were investigated. The rotamer with the lowest energy value was selected for subsequent calculations. The structures are shown in Figure S1 of the Supporting Information. Vibrational analysis obtained under the harmonic approximation at the B3LYP/6-31G* level has shown that the selected structures are minima in the PES (positive frequencies). Calculated geometries and relative

* Corresponding author phone: 0039-95-7385201; fax: 0039-95-580138; e-mail: vlibrando@dipchi.unict.it.

10.1021/es061632+ CCC: $37.00
Published on Web 01/24/2007

TABLE 1. Relative Energy, ΔE (kcal mol^{-1}), First Ionization Potential, IP (eV), and Hardness, η (eV), of Dimethylnaphthalene Isomers

		ΔE[a]			state	IP		η
compound	sym.	HF/6-31G*	MP2/6-31G*	B3LYP/6-31G*		calc.[b]	exp.	calc.[c]
1,2-DMN	C_s	4.37	2.19	3.37 (3.74)	$^2A''$	7.54		2.29
1,3-DMN	C_s	1.12	0.21	0.88 (1.08)	$^2A''$	7.57	7.86 [d]	2.34
1,4-DMN	C_s	2.61	0.72	1.97 (2.46)	$^2A_2$	7.54	7.82 [d]	2.28
1,5-DMN	C_{2h}	2.72	0.80	2.05 (2.54)	^2A_u	7.56	7.85 [d]	2.29
1,6-DMN	C_s	1.20	0.31	0.93 (1.14)	$^2A''$	7.58		2.34
1,7-DMN	C_s	1.30	0.26	0.93 (1.17)	$^2A''$	7.57		2.34
1,8-DMN	C_{2v}	9.93	7.02	8.23 (8.88)	$^2A_2$	7.49	7.71 [e]	2.31
2,3-DMN	C_{2v}	0.98	−0.03	0.58 (0.81)	$^2A_2$	7.60	7.89 [d]	2.37
2,6-DMN	C_{2h}	0.06	−0.03	0.03 (0.06)	^2A_u	7.57		2.38
2,7-DMN	C_{2v}	0.00	0.00	0.00 (0.00)	$^2A_2$	7.60	7.89 [d]	2.40
NPH					^2A_u	7.90	8.00 [f]	2.38

[a] Calculations are carried out on the geometry optimized at the specific level. Values in parentheses are corrected for zero-point vibrational energy. [b] Vertical ΔSCF values obtained at the B3LYP/6-31+G* level on the B3LYP/6-31G* geometry of the neutral ground state. [c] $\eta = (\epsilon_{LUMO} - \epsilon_{HOMO})/2$ obtained at the B3LYP/6-31+G* level on the B3LYP/6-31G* geometry of the neutral ground state. [d] Photoelectron spectroscopy (*66*). [e] Photoelectron spectroscopy (*67*). [f] Photoelectron spectroscopy (*68*).

energies of all the rotamers are available on request from the authors.

Dipole moment, μ, and static electronic dipole polarizability tensor components, α_{ij} (i = x, y, z), were computed analytically within the coupled-perturbed Hartree−Fock (CP−HF) theory, respectively, as first and second derivatives of the energy E with respect to the Cartesian components of the electric field F (*37*, *38*):

$$E(F) = E(0) - \sum_i \mu_i F_i - 1/2 \sum_{ij} \alpha_{ij} F_i F_j - \ldots \quad (1)$$

$$\alpha_{ij} = -\left[\frac{\partial^2 E(F)}{\partial F_i \partial F_j}\right]_{F\to 0} \quad (2)$$

Polarizability calculations were performed at the correlated B3LYP level using the 6-31G* as well as 6-31+G* basis sets (*32*), the last one including diffuse *s* and *p* functions on the carbon atoms. For the present compounds, 6-31G* and 6-31+G* basis sets give a total of 204 and 252 basis functions, respectively. It is well recognized that polarized and diffuse basis sets adequately describe the diffuse region of the charge distribution, becoming indispensable for accurate polarizability computations (*39*). In addition, polarizabilities are significantly influenced by introduction of electron correlation effects (*40*, *41*). It is well recognized that DFT methods are in trouble when dealing with polarizabilities of extended systems (*42*). However, there is much evidence showing that in molecular systems with limited π-conjugation, hybrid DFT methods give results of accuracy similar to those obtained by highest level correlated *ab initio* methods (*43*−*46*). Solute−solvent effects upon dipole moments and polarizabilities were taken into account within the framework of the polarizable continuum model (PCM) (*47*−*50*) in aqueous solution (ϵ = 78.39). Cavity radii were generated from the united atom model for Hartree−Fock, which has been employed with success in prediction of hydration free energies (*51*). PCM polarizability calculations were carried out on the gas-phase optimized geometry, since solvent geometric effects are expected to be negligible on polarizabilities, especially for nonpolar compounds, in comparison to those due to the solvent reaction field (*52*).

Polarizability is usually expressed in terms of arithmetic average of the three diagonal α_{ii} components:

$$< \alpha > = \frac{1}{3}(\alpha_{xx} + \alpha_{yy} + \alpha_{zz}) \quad (3)$$

Vertical electronic excitations to singlet valence states were computed through the time-dependent (TD) DFT method (*53*−*55*) at the B3LYP/6-31G* level on the B3LYP/6-31G* optimized geometry of the ground state.

Conversion factors to SI units are as follows: energy (E), 1 kcal mol^{-1} = 4.184 kJ mol^{-1}; dipole moment (μ), 1 Debye = 3.33564 × 10^{-30} Cm; dipole polarizability (α), 1 au = 1.648778 × 10^{-41} C^{2}m^{2}J^{-1}.

All calculations were performed with the Gaussian 03 package (*56*).

Results and Discussion

Relative Energies and Geometries. Table 1 shows the relative energies of DMN isomers which are true minima in the PES (no imaginary frequency). At the HF/6-31G* level of calculation the order of stability is 2,7-DMN ≈ 2,6-DMN > 2,3-DMN > 1,3-DMN ≈ 1,6-DMN ≈ 1,7-DMN > 1,4-DMN ≈ 1,5-DMN > 1,2-DMN > 1,8-DMN. Introduction of electron correlation effects at the MP2/6-31G* level reduces the relative energies by 1−3 kcal mol^{-1}; as a consequence, 2,3-DMN, 2,6-DMN, and 2,7-DMN become isoenergetic, while 1,3-DMN, 1,4-DMN, 1,5-DMN, 1,6-DMN, and 1,7-DMN lie less than 1 kcal mol^{-1} above the lowest isomer. The order of stability obtained by the B3LYP/6-31G* calculations is almost the same as at the HF/6-31G* and MP2/6-31G* levels, even if electron correlation contributions are of minor relevance in comparison with the MP2/6-31G* data. Introduction of zero-point vibrational corrections evaluated under the harmonic approximation at 298 K and 1 atm of pressure at the B3LYP/6-31G* level, decreases the stability of all the isomers by 0.03−0.65 kcal mol^{-1}, however maintaining the above order of stability. According to all the methods employed in this work, owing to the presence of strong steric hindrance between the methyl groups, 1,8-DMN is predicted to be the less stable isomer—the energy difference with respect to 2,7-DMN being 9.93, 7.05, and 8.23 kcal mol^{-1} at the HF/6-31G*, MP2/6-31G*, and B3LYP/6-31G* levels, respectively. It is of interest to note that with reference to experimental gas-phase standard enthalpy of formation for 1,8-DMN (*57*) and 2,7-DMN (*58*), which are 26.00 ± 0.72 and 19.00 ± 0.14 kcal mol^{-1}, respectively, a relative enthalpy value of 7.00 kcal mol^{-1} is obtained, to be compared with the corresponding B3LYP/6-31G* value of 8.61 kcal mol^{-1}, as well as with estimated HF/6-31G* and MP2/6-31G* values obtained using the B3LYP/6-31G* thermodynamic corrections which are 10.31 and 7.40 kcal mol^{-1}, respectively.

Optimized geometric parameters of DMN isomers (see Figure S1 of the Supporting Information for atomic number-

TABLE 2. Averaged Electronic Dipole Polarizabilities, <α> (au), Dipole Moment, μ (Debyes), and Atomic Polar Tensor Atomic Charges over Methyl Group, q(CH_3) (e) of Dimethylnaphthalene Isomers[a]

	<α>		μ	$q(CH_3)_\alpha$	$q(CH_3)_\beta$	
basis set	6-31G*	6-31+G*	6-31+G*	6-31G*	6-31G*	k_b[b]
compound						
1,2-DMN	124.19	142.39 (198.40)	0.71 (0.93)	0.01567	0.00837	0.10 ± 0.03
1,3-DMN	125.00	143.30 (199.19)	0.55 (0.74)	0.01822	−0.00056	0.12 ± 0.04
1,4-DMN	123.38	141.49 (197.56)	0.08 (0.08)	0.01860		0.055 ± 0.02
1,5-DMN	123.18	141.59 (197.82)	0.00 (0.00)	0.02301		0.065 ± 0.01
1,6-DMN	125.17	143.36 (199.04)	0.49 (0.68)	0.02083	0.00272	0.12 ± 0.04
1,7-DMN	124.96	143.21 (199.18)	0.62 (0.85)	0.02186	−0.00024	
1,8-DMN	122.59	140.61 (197.27)	0.66 (0.92)	0.00936		0.033 ± 0.02
2,3-DMN	126.31	144.30 (200.32)	0.91 (1.27)		−0.00089	
2,6-DMN	127.67	145.62 (200.69)	0.00 (0.00)		−0.00086	0.20 ± 0.05
2,7-DMN	127.44	145.55 (200.74)	0.21 (0.27)		−0.00064	0.36 ± 0.07
NPH [c]	98.95	116.34 (162.96)	0.00 (0.00)			

[a] All calculations are carried out at the B3LYP level on the B3LYP/6-31G* geometry. Values in parentheses refer to aqueous solution estimates. [b] Experimental first-order biomass-normalized rate coefficient (mg of protein/L)$^{-1}$(h)$^{-1}$ in aqueous systems (*19*). [c] <α>(HF/6-31+G*) = 111.39 a.u.; <α>(MP2/6-31+G*) = 113.68 a.u.; <α>(exp.) = 117.4 au from Laser Stark spectroscopy measurements in gas phase (*61, 62*).

ing), together with those of naphthalene (NPH), obtained at the B3LYP/6-31G* level of calculation are given in Table S1 of the Supporting Information and compared to available experimental data. The HF/6-31G* and MP2/6-31G* geometries are not reported in the table but are available on request from the authors. For NPH, all the computed geometries are in acceptable agreement with the experimental data obtained from electron diffraction measurements (*59*), with a root mean squared (rms) deviation for bond lengths of 0.012, 0.010, and 0.011 Å, respectively, for HF/6-31G*, MP2/6-31G*, and B3LYP/6-31G* levels. Note that the characteristic $C_1-C_9-C_8$ bond angle is nicely reproduced by all the theoretical methods within ca. 1°. In particular, note that correlated MP2/6-31G* and B3LYP/6-31G* geometries are close to each other. For 1,8-DMN isomer, neutron diffraction structures in the 50−200 K range of temperatures have been recently published (*60*). Present geometries, especially those at the correlated level, are in satisfactory agreement with experiment, with rms errors for bond distances of 0.017, 0.006, and 0.007 Å, at the HF/6-31G*, MP2/6-31G*, and B3LYP/6-31G* levels, respectively. Note also that $C_1-C_9-C_8$ and $C_4-C_{10}-C_5$ bond angles are well reproduced in particular by the correlated computations (within 0.6°).

It is of interest to investigate geometric effects on the NPH moiety of DMN isomers obtained by introduction of methyl substituents. As expected, the most remarkable structural effects are found for 1,8-DMN isomer with an rms deviation from the NPH bond lengths of 0.012 Å at the B3LYP/6-31G* level. In addition, in passing from NPH to 1,8-DMN, $C_1-C_9-C_8$ bond angle increases by 3.5°, while $C_4-C_{10}-C_5$ bond angle decreases by 3.9°. On the other hand, 2,7-DMN isomer exhibits a structure very close to that of NPH, with an rms deviation of 0.003 Å for bond distances and a variation of only 0.1° for the $C_1-C_9-C_8$ and $C_4-C_{10}-C_5$ bond angles. It is worth noting that for 1,8-DMN and 1,2-DMN isomers, where steric hindrance effects are maximized, $C-CH_3$ bond distances elongate by 0.007 and 0.003−0.006 Å, respectively, with respect to the related bonds in 2,7-DMN isomer.

Polarizabilities. Static averaged electronic dipole polarizabilities, <α> of DMN isomers in gas phase and aqueous solution are collected in Table 2. Computed <α> values of NPH, for which experimental estimates are available (*61*, *62*) are also included in the table. The results show that for NPH, B3LYP/6-31G* <α> value underestimates the observed figure (117.4 au) by 18.45 au (15.7%), while the inclusion of diffuse functions (6-31G* → 6-31+G*) noticeably improves the agreement with the experiment, with a difference of only 1.06 au (0.9%). As expected, introduction of electron correlation contributions at the MP2/6-31+G* and B3LYP/6-31+G* levels gives non-negligible positive corrections to the HF/6-31+G* polarizabilities (see footnote to Table 2), increasing <α> values by 2.1 and 4.4%, respectively, providing a better agreement with the experiment.

For DMN isomers, substitution of two hydrogen atoms with two methyl groups increases the polarizability of NPH by 25−38 au (22−23%), depending on the isomer and on the phase. As can be seen from Table 2, the gas-phase B3LYP/6-31+G* <α> value of DMN isomers increases in the order 1,8-DMN < 1,4-DMN ≈ 1,5-DMN < 1,2-DMN < 1,7-DMN ≈ 1,3-DMN ≈ 1,6-DMN < 2,3-DMN < 2,7-DMN ≈ 2,6-DMN, the largest difference being calculated to be ca. 5 au (3.5%). A similar trend occurs also for the B3LYP/6-31G* <α> values. The above polarizability comparison is suitable since the considered molecules have the same number and type of atoms, that is, they are isomers. Introduction of solvation effects which in absence of strong specific solute−solvent interactions can be properly accounted by the PCM method, increases steadily the gas phase <α> values by ca. 40%, the order of <α> in the series remaining almost unchanged. Note that the electronic polarizability of the investigated series is remarkably influenced by the position of the methyl substituents. In fact, the smallest <α> values are found for isomers with both the CH_3 functional groups in position α (1,8-DMN, 1,4-DMN, and 1,5-DMN), intermediate values are obtained for α,β-isomers (1,2-DMN, 1,7-DMN, 1,3-DMN, and 1,6-DMN), and the largest <α> values are calculated for isomers methylated in β positions (2,3-DMN, 2,7-DMN, and 2,6-DMN). At all the theoretical levels, 1,8-DMN which is the less stable isomer, is also the less polarizable, while 2,6-DMN and 2,7-DMN which are the most stable isomers exhibit the largest <α> values in the series. Note that this result is in disagreement with the minimum polarizability principle (*63*), which states that any system should tend toward a state of minimum polarizability.

With reference to recent studies (*28*−*30*), in which calculated electronic polarizabilities of polychlorinated isomers have been related to ligand−receptor binding properties, present <α> values have been correlated with experimental biodegradation rates, expressed by first-order biomass-normalized rate coefficients, k_b, which are available for 1,2-DMN, 1,3-DMN, 1,4-DMN, 1,5-DMN, 1,6-DMN, 1,8-DMN, 2,6-DMN, and 2,7-DMN isomers in aqueous systems (*19*). The experimental k_b values are included in Table 2. The results show that when excluding the 2,7-DMN isomer the calculated averaged electronic dipole polarizabilities of DMN isomers are found to be in excellent linear correlation with the observed k_b values, as depicted in Figure 1. Note that use of gas-phase polarizabilities leads to qualitative conclusions

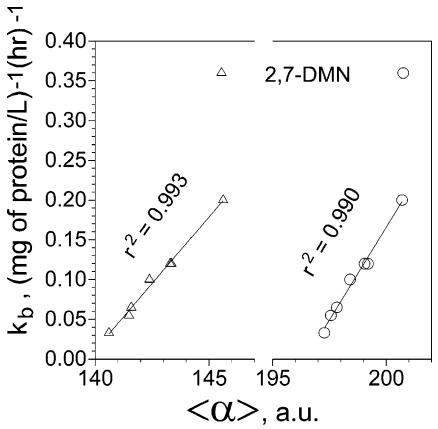

FIGURE 1. Relationship between the experimental biomass-normalized first-order rate coefficient, k_b (*19*) and the B3LYP/6-31+G* averaged electronic polarizability of 1,2-DMN, 1,3-DMN, 1,4-DMN, 1,5-DMN, 1,6-DMN, 1,8-DMN, 2,6-DMN, and 2,7-DMN isomers. Triangles and circles refer to gas and aqueous-phase values, respectively.

similar to those obtained using solvated values. As follows we report k_b vs <α> relationships, which may be useful for predictive purposes (r^2 = squared correlation coefficient, SD = standard deviation, P = probability):

$$k_b = (0.03231 \pm 0.00181) <\alpha> - (3.92254 \pm 0.22528),\ r^2 = 0.985,\ \mathrm{SD} = 0.00757,\ P < 10^{-4}$$
(B3LYP/6-31G* in gas phase) (4)

$$k_b = (0.03345 \pm 0.00127) <\alpha> - (4.67214 \pm 0.18160),\ r^2 = 0.993,\ \mathrm{SD} = 0.00516,\ P < 10^{-4}$$
(B3LYP/6-31+G* in gas phase) (5)

$$k_b = (0.04673 \pm 0.00211) <\alpha> - (9.17991 \pm 0.41896),\ r^2 = 0.990,\ \mathrm{SD} = 0.00612,\ P < 10^{-4}$$
(B3LYP/6-31+G* in aqueous solution) (6)

On the other hand, when we exclude 2,6-DMN and include 2,7-DMN in the k_b vs <α> relationships, the squared correlation coefficients worsen (r^2 = 0.94 at the B3LYP/6-31+G* in the gas phase). It must be mentioned that 2,7-DMN shows the most uncertain k_b value in the series (0.36 ± 0.07) (*19*). Current calculations for 2,6-DMN and 2,7-DMN isomers give very close polarizability values (145.62 and 145.55 au, respectively, at the B3LYP/6-31+G* level in the gas phase) as well as similar stability (Table 1), although they exhibit somewhat different k_b values (0.20 ± 0.05 and 0.36 ± 0.07, for 2,6-DMN and 2,7-DMN, respectively) (*19*). Note that, however, these β,β-DMN isomers have rather different aqueous solubility (1.7 and 14.9 mg/L, for 2,6-DMN and 2,7-DMN, respectively) (*19*), difference in dipole moment value (see Table 2), and 2,6-DMN is slightly bulkier than 2,7-DMN (*64*). These factors together with a noticeable uncertainty in the experimental measurements may be responsible of their different k_b values. The above results suggest that both inductive and dispersive interactions of DMNs with active site residues of PAH-degrading enzyme play a crucial role in the biodegradation process. In the hypothesis that eqs 4−6 are valid, they may be used to predict k_b value of 1,7-DMN and 2,3-DMN isomers for which observed values are unavailable, and also tentatively to furnish an estimate for 2,7-DMN isomer. With the use of <α> values reported in Table 2, the k_b values evaluated through eq 6 for 1,7-DMN, 2,3-DMN, and 2,7-DMN isomers are 0.13, 0.20, and 0.20 (mg of protein/L)$^{-1}$(h)$^{-1}$, respectively.

Ionization Potential, Hardness, and Lowest Energy Electronic Transitions. Electronic polarizabilities have often been associated with molecular hardness, η, a widely used parameter which represents a measure of the stability of a molecular system (*65*). Hardness is usually approximated by (IP − EA)/2 ≈ ($\epsilon_{LUMO} - \epsilon_{HOMO}$)/2 expressions, where IP, EA, ϵ_{HOMO}, and ϵ_{LUMO} are the first ionization potential, electron affinity, highest occupied molecular orbital (HOMO), and lowest unoccupied molecular orbital (LUMO) eigenvalues, respectively. Table 1 reports η and IP values of DMN, as well as those of NPH for comparison. B3LYP/6-31+G* IP values underestimate the observed figures obtained from X-ray photoelectron spectroscopy measurements (*66*−*68*) by 0.1−0.3 eV (1−4%). Note that introduction of methyl substituents to the NPH moiety decreases IP value of DMN isomers by 0.3−0.4 eV, owing to the antibonding character of the σ-(CH_3)-π(NPH) hyperconjugative interaction which destabilizes ϵ_{HOMO} (under the Koopman's approximation, IP ≈ $-\epsilon_{HOMO}$). As can be seen in Table 1, IP slightly varies along the series of DMN conformations (0.11 eV), with the lowest and the highest values being found for 1,8-DMN and 2,7-DMN (2,3-DMN) isomers, respectively, at 7.49 and 7.60 eV at the B3LYP/6-31+G* level, in reasonable agreement with experiment. Thus, despite that the biodegradation reactions involve an electrophilic attack on DMNs (*19*, *21*), this result suggests that the first ionization process does not play a fundamental role in the biodegradation pathway of this series of compounds. As for IP, also η varies little in the series (0.12 eV). However, it is interesting to notice that η is maximized in β,β-DMN isomers (2.37−2.40 eV for 2,3-DMN, 2,6-DMN, and 2,7-DMN), whereas it shows lower values in α,α-DMN isomers (2.29−2.31 eV for 1,2-DMN, 1,4-DMN, 1,5-DMN, 1,8-DMN) in reasonable consistency with the computed stabilities (Table 1), the maximum hardness principle (*69*), which states that molecules arrange themselves so as to be hard as possible in the present case being satisfied.

Under the sum-over-states (SOS) formalism, in the static limit, electronic dipole polarizability components α_{ii} are related to excitation energy, E^{ng}, and electronic transition moment along i direction from the ground to the n excited state, M_i^{ng} as (*70*, *71*):

$$\alpha_{ii} = 2 \sum_n \frac{(M_i^{ng})^2}{E^{ng}} \quad (7)$$

It is worth noting that the most intense electronic transition for DMN isomers which occurs at ca. 5.9 eV (oscillator strengths in the 0.8−1.4 au range, see Table S2 of the Supporting Information), gives through eq 7 the largest contribution to <α> (50−60%), while the lowest energy excitation, which is located at about 4.3−4.4 eV in reasonable agreement with experiment (*72*), does not substantially contribute to <α> values, owing to the low intensity which is about 1 order of magnitude smaller than that of the most intense absorption.

Following the SOS results, it could be interesting to investigate the origins of the difference of <α> values between 1,8-DMN and 2,6-DMN isomers. Figure 2 depicts the simulated absorption spectra of 1,8-DMN and 2,6-DMN isomers in the 4−7 eV energy range which include the lowest ten singlet electronic excitations. As shown in the figure, for both the isomers the strongest absorption occurs at about the same energy value of 5.87 eV corresponding to a wavelength λ of 211 nm; nevertheless, these bands differ substantially in intensity being ca. 40% greater in the 2,6-DMN isomer. For 1,8-DMN and 2,6-DMN isomers, these transitions mainly originate from the valence HOMO-1($4b_1$) → LUMO($4a_2$) and HOMO($4a_u$) → LUMO+1($5b_g$) excitations, respectively. For 2,6-DMN isomer both HOMO and LUMO+1

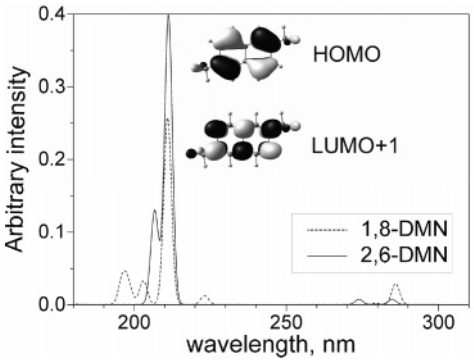

FIGURE 2. Gas-phase TD-B3LYP/6-31G* absorption spectra of 1,8-DMN and 2,6-DMN isomers and B3LYP/6-31G* HOMO and LUMO+1 molecular orbitals of 2,6-DMN isomer. Gaussian line shapes with half width of 3 nm are used.

(see Figure 2) are principally localized on the π NPH moiety, with the additional non-negligible σ contribution from the methyl groups; on the other hand, for the HOMO-1 of 1,8-DMN isomer the $\sigma-\pi$ interaction is lacking. It is also important to notice that at variance of 1,8-DMN isomer, for 2,6-DMN another relevant excited-state contribution to the polarizability is provided from the intense absorption at 6.0 eV (oscillator strength of 0.4 au at $\lambda = 207$ nm), which mainly originates from the HOMO-1($3a_u$) → LUMO+1($5b_g$) excitation.

Atom Charges and Dipole Moments. Atomic charges of the investigated DMN isomers were evaluated according to the atomic polar tensor (APT) method (*73*, *74*). The sum of the APT charges over the methyl group, q(CH_3), computed at the B3LYP/6-31G* are listed in Table 2. For all the isomers q(CH_3) is close to zero. As can be seen in the Table, for 1,8-DMN q(CH_3) is positive, while for both 2,6- and 2,7-DMN isomers it is slightly negative. This result shows that despite IP(1,8-DMN) < IP(2,6-DMN) ≈ IP(2,7-DMN) (Table 1), CH_3 groups of 2,6-DMN and 2,7-DMN isomers are more susceptible toward electrophilic attacks than those of 1,8-DMN isomer, favoring the oxidation step of the biodegradation process. Note that with reference to the q(CH_3) charges of 1,2-DMN, 1,3-DMN, 1,6-DMN, 1,7-DMN isomers, the monooxygenative attack on methyl groups should be preferred in the β position.

Table 2 gives dipole moments of the investigated DMN congeners obtained in gas phase and aqueous solution at the B3LYP/6-31+G* level. As can be seen from the table, dipole moments are somewhat small, consistently with the low q(CH_3) charges, with the largest value being found for 2,3-DMN (0.91 Debyes in gas phase). Other relatively moderate values are also found for 1,2-DMN and 1,8-DMN isomers, which, as for 2,3-DMN isomer, have the methyl groups vicinal to each other. The order of the computed μ values is 1,5-DMN = 2,6-DMN < 1,4-DMN < 2,7-DMN < 1,6-DMN < 1,3-DMN < 1,7-DMN < 1,8-DMN < 1,2-DMN < 2,3-DMN. Solvation effects increase gas-phase values by 0.06−0.36 Debyes. However, it is worth noting that despite non-negligible solvation effects on both μ and α, solute−solvent interactions do not furnish substantial changes in the stability order of the DMN isomers.

Acknowledgments

This work was partially supported by MIUR, Rome, and COMETA Consortium (Consorzio Multi Ente per la Promozione e l'Adozione di Tecnologie di Calcolo Avanzato), Catania.

Supporting Information Available

One figure depicting molecular structures and atomic numbering (Figure S1), two tables of geometries (Table S1) and singlet excitation energy and oscillator strength data (Table S2). This material is available free of charge via the Internet at http://pubs.acs.org.

Literature Cited

(1) Librando, V.; Fazzino, D. S. The quantification of polycyclic aromatic hydrocarbons and their nitro-derivatives in the atmospheric particulate matter of Augusta city. *Chemosphere* **1993**, *27*, 1649−1654.
(2) Castelli, F.; Librando, V.; Sarpietro, M. G. A calorimetric approach of the interaction and absorption of polycyclic aromatic hydrocarbons with model membranes. *Environ. Sci. Technol.* **2002**, *36*, 2717−2723.
(3) Hoffmann, D; Wynder, E. L. In *Air Pollution*; Stern, A. C., Ed.; Academic Press: New York, 1977; vol. 2, pp 361−455.
(4) Nordquist, M.; Thakker, D. R.; Yagi, H.; Lehr, R. E.; Wood, A. W.; Levin, W.; Conney, A. H.; Jerina, D. M. In *Molecular Basis of Environmental Toxicity*; Bhatnagar, R. S., Ed.; Ann Arbor Science Publishers: Ann Arbor, MI, 1980; pp 329−357.
(5) Harvey, R. G. In *Polycyclic Aromatic Hydrocarbons: Chemistry and Carcinogenicity*; Cambridge University Press: Cambridge, UK, 1991.
(6) Motta, S.; Federico, C.; Saccone, S.; Librando, V.; Mosesso, P. Cytogenetic evaluation of extractable agents from airborne particulate matter generated in the city of Catania (Italy). *Mutat. Res.* **2004**, *561*, 45−52.
(7) Puget, J. L.; Leger, A.; Boulanger, F. Contribution of large polycyclic aromatic molecules to the infrared emission of the interstellar medium. *Astron. Astrophys.* **1985**, *142*, L19−L22.
(8) Allamandola, L. J. Benzenoid hydrocarbons in space: the evidence and implications. *Topics Curr. Chem.* **1990**, *153*, 1−25.
(9) Szczepanski, J.; Vala, M. Laboratory evidence of ionized polycyclic aromatic hydrocarbons in the interstellar medium. *Nature* **1993**, *363*, 699−701.
(10) Librando, V.; Castelli, F.; Sarpietro, M. G.; Aresta, M. *Sequential Reactivity Studies Of B[A]P And B[E]P By Chemical And Biological Processes, In situ and On-Site Bioremediation*; Battelle Press: Columbus, OH, 2002.
(11) Librando, V.; Forte, S. Computer assisted evaluation of protein segments removal effects from naphthalene 1,2-dioxygenase enzyme on polycyclic aromatic hydrocarbons interaction. *J. Chem. Technol. Biotechnol.* **2005**, *27*, 161−166.
(12) Peters, C. A.; Luthy, R. G. Coal-tar dissolution in water-miscible solvents − experimental evaluation. *Environ. Sci. Technol.* **1993**, *27*, 2831−2843.
(13) Garcia, K. L.; Delfino, J. J.; Powell, D. H. Non-regulated organic compounds in Florida sediments. *Water Res.* **1993**, *27*, 1601−1613.
(14) Burkhard, L. P.; Sheedy, B. R. Evaluation of screening procedures for bioconcentratable organic chemicals in effluents and sediments. *Environ. Toxicol. Chem.* **1995**, *14*, 697−711.
(15) Solanas, A. M.; Pares, R.; Bayona, J. M.; Albaiges, J. Degradation of aromatic petroleum-hydrocarbons by pure microbial cultures. *Chemosphere* **1984**, *13*, 593−601.
(16) Volkman, J. K.; Alexander, R.; Kagi, R. I.; Rowland, S. J.; Sheppard, P. N. Biodegradation of aromatic hydrocarbons in crude oils from the barrow sub-basin of western australia. *Org. Geochem.* **1984**, *6*, 619−632.
(17) Bayona, J. M.; Albaiges, J.; Solanas, A. M.; Pares, R.; Garrigues, P.; Ewald, M. Selective aerobic degradation of methyl-substituted polycyclic aromatic hydrocarbons in petroleum by pure microbial cultures. *Int. J. Environ. Anal. Chem.* **1986**, *23*, 289−303.
(18) Bastow, T. P.; van Aarssen, B. G. K.; Alexander, R.; Kagi, R. I. Biodegradation of aromatic land-plant biomarkers in some australian crude oils. *Org. Geochem.* **1999**, *30*, 1229−1239.
(19) Wammer, K. H.; Peters, C. A. Polycyclic aromatic hydrocarbon biodegradation rates: a structure-based study. *Environ. Sci. Technol.* **2005**, *39*, 2571−2578.
(20) Selifonov, S. A.; Grifoll, M.; Eaton, R. W.; Chapman, P. J. Oxidation of naphthenoaromatic and methyl-substituted aromatic compounds by naphthalene 1,2-dioxygenase. *Appl. Environ. Microbiol.* **1996**, *62*, 507−514.
(21) Wammer, K. H.; Peters, C. A. A molecular modeling analysis of polycyclic aromatic hydrocarbon biodegradation by naphthalene dioxygenase. *Environ. Toxicol. Chem.* **2006**, *25*, 912−920.
(22) Buckingham, A. D. Permanent and induced molecular moments and long-range intermolecular forces. *Adv. Chem. Phys.* **1967**, *12*, 107−142.
(23) Bogard, M. P.; Orr, B. J. In *Physical Chemistry, Series Two, Vol. 2. Molecular Structure and Properties*; Buckingham, A. D., Ed.; Butterworths: London, 1975.

(24) Miller, K. J. Additivity methods in molecular polarizability. *J. Am. Chem. Soc.* **1990**, *112*, 8533−8542.
(25) Miller, T. M. *CRC Handbook of Chemistry and Physics*, 77th ed.; CRC Press: Boca Raton, FL, 1996−97.
(26) Butcher, P. N.; Cotter, D. *The Elements of Nonlinear Optics*; Cambridge, University Press, UK, 1991.
(27) Dykstra, C. E. *Ab initio Calculation of the Structure and Properties of Molecules*; Elsevier: Amsterdam, 1985.
(28) Fraschini, E.; Bonati, L.; Pitea, D. Molecular polarizability as a tool for understanding the binding properties of polychlorinated dibenzo-*p*-dioxins: definition of a reliable computational procedure. *J. Phys. Chem.* **1996**, *100*, 10564−10569.
(29) Mhin, B. J.; Lee, J. E.; Choi, W. Understanding the congener-specific toxicity in polychlorinated dibenzo-*p*-dioxins: chlorination pattern and molecular quadrupole moment *J. Am. Chem. Soc.* **2002**, *124*, 144−148.
(30) Hirokawa, S.; Imasaka, T.; Imasaka, T. Chlorine substitution pattern, molecular electronic properties, and the nature of the ligand-receptor interaction: quantitative property-activity relationships of polychlorinated dibenzofurans. *Chem. Res. Toxicol.* **2005**, *18*, 232−238.
(31) Staikova, M.; Wania, F.; Donaldson, D. J. Molecular polarizability as a single-parameter predictor of vapour pressures and octanol−air partitioning coefficients of non-polar compounds: a priori approach and results. *Atmos. Environ.* **2004**, *38*, 213−225.
(32) Hehre, W. J.; Random, L.; Schleyer, P. v. R.; Pople, J. A. *Ab Initio Molecular Orbital Theory*; Wiley: New York, 1986.
(33) Kohn, W.; Sham, L. J. Self-consistent equations including exchange and correlation effects. *Phys. Rev. A* **1965**, *140*, 1133−1138.
(34) Parr, R. G.; Yang, W. *Density Functional Theory of Atoms and Molecules;* Oxford University Press: New York, 1989.
(35) Lee, C.; Yang, W.; Parr, R. G. Development of the Colle-Salvetti correlation energy formula into a functional of the electron density. *Phys. Rev. B* **1988**, *37*, 785−789.
(36) Becke, A. D. Density-functional thermochemistry. III. The role of exact exchange. *J. Chem. Phys.* **1993**, *98*, 5648−5652.
(37) Sekino, H.; Bartlett, R. J. Frequency dependent nonlinear optical properties of molecules. *J. Chem. Phys.* **1986**, *85*, 976−989.
(38) Karna, S. P.; Dupuis, M. Frequency dependent nonlinear optical properties of molecules: formulation and implementation in the HONDO program. *J. Comput. Chem.* **1991**, *12*, 487−504.
(39) Rice, J. E.; Handy, N. C. The calculation of frequency-dependent polarizabilities as pseudo-energy derivatives. *J. Chem. Phys.* **1991**, *94*, 4959−4971.
(40) Rice, J. E.; Amos, R. D.; Colwell, S. M.; Handy, N. C.; Sanz, J. Frequency dependent hyperpolarizabilities with application to formaldehyde and methyl fluoride. *J. Chem. Phys.* **1990**, *93*, 8828−8839.
(41) Sekino, H.; Bartlett., R. J. Molecular hyperpolarizabilities. *J. Chem. Phys.* **1993**, *98*, 3022−3037.
(42) Champagne, B.; Perpete, E. A.; van Gisbergen, S. J. A.; Baerends, E.-J.; Snijders, J. G.; Soubra-Ghaoui, C.; Robins, K. A.; Kirtman, B. Assessment of conventional density functional schemes for computing the polarizabilities and hyperpolarizabilities of conjugated oligomers: An ab initio investigation of polyacetylene chains. *J. Chem. Phys.* **1998**, *109*, 10489−10498.
(43) Millefiori, S.; Alparone, A. Ab initio and density functional theory calculations of the dipole polarizabilities of ethene, benzene and naphthalene. *J. Mol. Struct. (Theochem)* **1998**, *422*, 179−190.
(44) Millefiori, S.; Alparone, A. Tautomerism and polarizability in uracil: coupled cluster and density-functional theory study. *Chem. Phys.* **2004**, *303*, 27−36.
(45) Alparone, A.; Millefiori, A.; Millefiori, S. Non-planarity and solvent effects on structural and polarizability properties of cytosine tautomers. *Chem. Phys.* **2005**, *312*, 261−274.
(46) Alparone, A.; Reis, H.; Papadopoulos, M. G. Theoretical investigation of the (hyper)polarizabilities of pyrrole homologues C_4H_4XH (X = N, P, As, Sb, Bi). A coupled-cluster and density functional theory study. *J. Phys. Chem. A* **2006**, *110*, 5909−5918.
(47) Miertus, S.; Scrocco, E.; Tomasi, J. Electrostatic interaction of a solute with a continuum. A direct utilization of *ab initio* molecular potentials for the prevision of solvent effects. *Chem. Phys.* **1981**, *55*, 117−129.
(48) Tomasi, J.; Persico, M. Molecular interactions in solution: an overview of methods based on continuous distributions of the solvent. *Chem. Rev.* **1994**, *94*, 2027−2094.
(49) Cammi, R.; Tomasi, J. Remarks on the use of the apparent surface charges (ASC) methods in solvation problems: Iterative versus matrix-inversion procedures and the renormalization of the apparent charges. *J. Comput. Chem.* **1995**, *16*, 1449−1458.
(50) Cossi, M.; Scalmani, G.; Rega, N.; Barone, V. New developments in the polarizable continuum model for quantum mechanical and classical calculations on molecules in solution. *J. Chem. Phys.* **2002**, *117*, 43−54.
(51) Barone, V.; Cossi, M.; Tomasi, J. A new definition of cavities for the computation of solvation free energies by the polarizable continuum model. *J. Chem. Phys.* **1997**, *107*, 3210−3221.
(52) Mennucci, B.; Cammi, R.; Cossi, M.; Tomasi, J. Solvent and vibrational effects on molecular electric properties. Static and dynamic polarizability and hyperpolarizabilities of urea in water. *J. Mol. Struct. (Theochem)* **1998**, *426*, 191−198.
(53) Bauernschmitt, R.; Ahlrichs, R. Treatment of electronic excitations within the adiabatic approximation of time dependent density functional theory. *Chem. Phys. Lett.* **1996**, *256*, 454−464.
(54) Casida, M. E.; Jamorski, C.; Casida, K. C.; Salahub, D. R. Molecular excitation energies to high-lying bound states from time-dependent density-functional response theory: characterization and correction of the time-dependent local density approximation ionization threshold. *J. Chem. Phys.* **1998**, *108*, 4439−4449.
(55) Stratmann, R. E.; Scuseria, G. E.; Frisch, M. J. An efficient implementation of time-dependent density-functional theory for the calculation of excitation energies of large molecules. *J. Chem. Phys.* **1998**, *109*, 8218−8224.
(56) Frisch, M. J.; Trucks, G. W.; Schlegel, H. B.; Scuseria, G. E.; Robb, M. A.; Cheeseman, V. G.; Montgomery, J. A.; Vreven, T., Jr.; Kudin, K. N.; Burant, J. C.; Millam, J. M.; Iyengar, S. S.; Tomasi, J.; Barone, V.; Mennucci, B.; Cossi, M.; Scalmani, G.; Rega, N.; Petersson, G. A.; Nakatsuji, H.; Hada, M.; Ehara, M.; Toyota, K.; Fukuda, R.; Hasegawa, J.; Ishida, M.; Nakajima, T.; Honda, Y.; Kitao, O.; Nakai, H.; Klene, M.; Li, X.; Knox, J. E.; Hratchian, H. P.; Cross, J. B.; Adamo, C.; Jaramillo, J.; Gomperts, R.; Stratmann, R. E.; Yazyev, O.; Austin, A. J.; Cammi, R.; Pomelli, C.; Ochterski, J. W.; Ayala, P. Y.; Morokuma, K.; Voth, G. A.; Salvador, P.; Dannenberg, J. J.; Zakrzewski, V. G.; Dapprich, S.; Daniels, A. D.; Strain, M. C.; Farkas, O.; Malick, D. K.; Rabuck, A. D.; Raghavachari, K.; Foresman, J. B.; Ortiz, J. V.; Cui, Q.; Baboul, A. G.; Clifford, S.; Cioslowski, J.; Stefanov, B. B.; Liu, G.; Liashenko, A.; Piskorz, P.; Komaromi, I.; Martin, R. L.; Fox, D. J.; Keith, T.; Al-Laham, M. A.; Peng, C. Y.; Nanayakkara, A.; Challacombe, M.; Gill, P. M. W.; Johnson, B.; Chen, W.; Wong, M. W.; Gonzalez, C.; Pople, J. A. *Gaussian 03*, revision A.1; Gaussian, Inc.: Pittsburgh, PA, 2003.
(57) Mansson, M. A calorimetric study of peri strain in 1,8-Dimethylnaphthalene and 1,4,5,8-Tetramethylnaphthalene. *Acta Chem. Scand. Ser. B* **1974**, *28*, 677−680.
(58) Chirico, R. D.; Knipmeyer, S. E.; Nguyen, A.; Steele, W. V. The thermodynamic properties to the temperature 700 K of naphthalene and of 2,7-dimethylnaphthalene. *J. Chem. Thermodyn.* **1993**, *25*, 1461−1494.
(59) Almenningen, A.; Bastiansen, O.; Dyvik, F. An attempt to determine the structure parameters of condensed-ring hydrocarbons by the electron-diffraction method in gas molecules. *Acta Crystallogr.* **1961**, *14*, 1056−65.
(60) Wilson, C. C.; Nowell, H. Methyl group librations in sterically hindered dimethylnaphthalene molecules: neutron diffraction studies of 1,8-dimethylnaphthalene between 50 and 200 K. *New J. Chem.* **2000**, *24*, 1063−1066.
(61) Heitz, S.; Weidauer, D.; Hese, A. On the polarizabilities of centrosymmetric molecules: naphthalene as an example. *Chem. Phys. Lett.* **1991**, *176*, 55−60.
(62) Heitz, S.; Weidauer, D.; Rosenow, B.; Hese, A. Measurement of static polarizabilities on naphthalene and naphthalene-d_8 ($C_{10}H_8$ and $C_{10}D_8$). *J. Chem Phys.* **1992**, *96*, 976−981.
(63) Chattaraj, P. K.; Sengupta, S. Popular electronic structure principles in a dynamical context. *J. Phys. Chem.* **1996**, *100*, 16126−16130.
(64) Fang, Y.; Hu, H. Shape-selectivity in 2,6-dimethylnaphthalene synthesis over ZSM-5: computational analysis using density functional theory. *Catal. Commun.* **2006**, *7*, 264−267.
(65) Parr, R. G.; Pearson, R. G. Absolute hardness: companion parameter to absolute electronegativity. *J. Am. Chem. Soc.* **1983**, *105*, 7512−7516.
(66) Heilbronner, E.; Hoshi, T.; von Rosenberg, J. L.; Hafner, K. Alkyl-induced, natural hypsochromic shifts of the $^2A \leftarrow {}^2X$ and $^2B \leftarrow {}^2X$ transitions of azulene and naphthalene radical cations. *Nouv. J. Chim.* **1976**, *1*, 105−112.
(67) Guttenberger, H. G.; Bestmann, H. J.; Dickert, F. L.; Jorgensen, F. S.; Snyder, J. P. Sulfur-bridged peri-naphthalenes: Synthesis, conformational analysis, and photoelectron spectroscopy of the

mono-, di-, and trisulfides of 1,8-diethylnaphthalene. *J. Am. Chem. Soc.* **1981**, *103*, 159−168.
(68) Yamauchi, M.; Yamakita, Y.; Yamakado, H.; Ohno, K. Collision energy resolved Penning ionization electron spectra of polycyclic aromatic hydrocarbons. *J. Electron Spectrosc. Relat. Phenom.* **1998**, *88*−*91*, 155−161.
(69) Pearson, R. G. The principle of maximum hardness. *Acc. Chem. Res.* **1993**, *26*, 250−255.
(70) Orr, B. J.; Ward, J. F. Perturbation theory of the non-linear optical polarization of an isolated system. *Mol. Phys.* **1971**, *20*, 513−526.
(71) Meyers, F.; Marder, S. R.; Pierce, B. M.; Bredas, J.-L. Electric Field Modulated Nonlinear Optical Properties of Donor-Acceptor Polyenes: Sum-Over-States Investigation of the Relationship between Molecular Polarizabilities (α, β, and γ) and Bond Length Alternation. *J. Am. Chem. Soc.* **1994**, *116*, 10703−10714.
(72) Mora-Diez, N.; Boyd, R. J.; Heard, G. L. Effects of alkyl substituents on the excited states of naphthalene: semiempirical study. *J. Phys. Chem. A* **2000**, *104*, 1020−1029.
(73) Person, W. B.; Newton, J. H. Dipole moment derivatives and infrared intensities. I. Polar tensors. *J. Chem. Phys.* **1974**, *61*, 1040−1049.
(74) Cioslowski, J. A new population analysis based on atomic polar tensors. *J. Am. Chem. Soc.* **1989**, *111*, 8333−8336.

Received for review July 10, 2006. Revised manuscript received December 15, 2006. Accepted January 3, 2007.

ES061632+